

# Transmission performance analysis of non-circular gear hydraulic motor

Yongping Liu\*, Xiangyu Ren, Changbin Dong

School of Mechanical and Electrical Engineering, Lanzhou University of Technology, Lanzhou 730050, P. R. China

Received 13 Apr 2024

Accepted 26 Jun 2024

## Abstract

The non-circular planetary gear train is a critical component of the hydraulic motor. It consists of internal and external non-circular gears with variable centre distance and several planetary gears. Transmission performance of the planetary gear train is considerable important to the overall structure analysis. In this research, two kinds of design methods are used for 6-8 type non-circular gear hydraulic motor. The high-order ellipse and double circular arc non-circular planetary gear train pitch curves are designed respectively. The influence of different modelling methods on the transmission performance of the whole planetary gear train are discussed. The results show that in the transmission process of the non-circular gear motor planetary gear train, the abrupt change of the planetary gear speed and the abrupt change of the rotational angular velocity of the planetary gear are located at the largest and smallest direction of the inner ring gear. The volume of each closed chamber of the motor changes at different times, resulting in the overall displacement pulsation. Under the same conditions, double arc type non-circular gear hydraulic motor than higher-order ellipse non-circular gear hydraulic motor in the same chamber work cycle can be in and out of more volume of oil, with better transmission smoothness.

© 2024 Jordan Journal of Mechanical and Industrial Engineering. All rights reserved

**Keywords:** Non-circular gear hydraulic motor, Planetary gear train, Higher-order ellipse, Double circular arc, Transmission performance.

## Nomenclature

$R_1$	Radial vector of sun gear [mm]
$R_2$	Planetary gear radius [mm]
$R_3$	Radial vector of inner ring gear [mm]
$\theta_1$	Polar Angle of sun gear [rad]
$\theta_2$	Polar Angle of inner ring gear [rad]
$A$	Radius of the long axis of the ellipse [mm]
$k$	Eccentricity of the ellipse
$m$	Modulus [mm]
$\mu_1$	Angle between the forward tangent of the curve of solar gear $R_1(\theta_1)$ pitch and radial vector $R_1$ [rad]
$z_1$	The number of teeth of sun gear
$z_2$	The number of teeth of planetary gear
$z_3$	The number of teeth of inner ring gear
$n_1$	The number of waves of the sun gear
$n_3$	The number of waves of the inner ring gear
$x_1$	Length of $OO_1$ [mm]
$y_1$	Length of $OO_1'$ [mm]
$r_1$	Length of $O_1C$ [mm]
$r_1'$	Length of $CO_1'$ [mm]
$x_2$	Length of $OO_2$ [mm]
$y_2$	Length of $OO_2'$ [mm]
$r_2$	Length of $O_2F$ [mm]
$r_2'$	Length of $FO_2'$ [mm]
$r_3$	Radius of the cylindrical planetary gear [mm]
$t$	Time [s]
$v_{m2}$	Velocity of the planet gear centroid [mm/s]
$v_{\theta 02}$	Rotation angular velocity of the planetary gear [mm/s]
$r_{o2}$	Radial vector of planetary gear [mm]
$\varphi_{o2}$	Rotation angle of the centroid of the planetary gear [rad]
$\omega_1$	Angular velocity of sun gear [rad/s]

$\omega_2$	Angular velocity of planetary gear [rad/s]
$\varphi_1$	Rotation angle of sun gear [rad]
$\varphi_2$	Rotation angle of planetary gear [rad]
$q_{max}$	Maximum instantaneous flow rate of the motor [mm <sup>2</sup> /s]
$q_{min}$	Minimum instantaneous flow rate of the motor [mm <sup>2</sup> /s]
$q_{av}$	Average flow rate of the motor [mm <sup>2</sup> /s]
$\delta_q$	Pulsation coefficient

## 1. Introduction

Hydraulic motors are widely used power devices that convert the pressure energy of hydraulic oil into mechanical energy to drive loads [1]. Among these devices, the non-circular gear hydraulic motor stands out as a novel hydraulic motor that combines gear motors with planetary gear trains. At its core lies the variable center distance non-circular gear planetary gear train mechanism, which boasts a simple structure, high efficiency, high torque at low speeds, excellent speed regulation performance, and robust pollution resistance [2]. Pitch curve design and teeth profile generation for non-circular planetary gear trains is one of the design difficulties [3]. Therefore, the analysis of transmission performance has become a crucial aspect.

Non-circular planetary gear trains are widely used in mechanical transmissions, including automotive transmissions, rotorcraft, wind and gas turbine gearboxes, and other Marine and industrial power trains [4]. A. Al-Shhyab et al. [5] according to the torsional dynamic characteristics of a typical multi-mesh gear train, they

\* Corresponding author e-mail: camelieu@163.com.

established a non-linear time-varying dynamic model. C. Dong et al.[6] simulated the dynamic meshing process of elliptical cylindrical gear planetary gear train commutator and studied the distribution of stress and strain during meshing at different speeds. A. Hammood [7] introduced the production of helical gear power conversion defect induction test bench and finite element analysis, and designed the optimal light gear transmission system.

The non-circular gear hydraulic motor planetary gear train in this research was first invented by Polish scholar B. Sieniawski which is called the satellite mechanism. There are currently two main design methods for modeling the planetary gear train of non-circular gear hydraulic motors: high-order ellipse and double circular arc. The higher-order ellipse method involves obtaining numerical solutions by exploiting the geometric kinematic relationships between the planetary gear train, which are fitted into higher-order ellipses. R. Jasiński [8] established a higher-order ellipse type non-circular gear hydraulic motor and analyzed the temperature field distribution of the motor during heating startup, thereby determining the operating conditions under actual working conditions. B. Zhanget al.[9] proposed a calculation method to determine the motion characteristics of the planetary gear train in a higher-order ellipse type non-circular gear hydraulic motor during transmission. This method involves augmenting the original equation of the sun gear pitch curve with an optimization factor to derive the optimized equation. P. Sliwinski[10]-[12] proposed a planetary gear train design approach based on the sine function, which utilizes the helix line of the sun gear. N. Shi et al.[13] analyzed the manufacturing process for non-circular gear hydraulic motors. They modeled the three-dimensional parameters of the high-order ellipse of the planetary gear train in non-circular gear hydraulic motors parametrically, using teeth envelope rolling and teeth profile smoothing techniques.

The double circular arc method involves using two segments of different smooth transition circular arcs to replace a portion of the pitch curve. This results in obtaining the entire non-circular gear pitch curve through an array. D. Li et al.[14] developed a nonlinear programming model for circular arc pitch curves and designed a 4-6 type non-circular planetary gear double circular arc mechanism with a module of 1.5. C. Song et al.[15] proposed a method for designing double circular arc profiles for harmonic gears using curve mapping and bidirectional conjugation. W. Zhang et al.[16] developed a model for a hydraulic motor featuring a double circular arc non-circular gear. They analyzed the leakage between the planetary gear train and the flow distribution plate of the hydraulic motor using fluid mechanics.

Currently, research primarily focuses on studying non-circular planetary gear trains, with relatively few studies on the transmission performance of non-circular gear hydraulic motors. Therefore, by analyzing the motion characteristics of high-order ellipse and double arc non-circular gear hydraulic motors, the motion rules and flow distribution rules of the two kinds of motors are investigated, so as to obtain non-circular gear hydraulic motors with better transmission performance.



Figure 1. The physical picture of 6-8 type non-circular gear hydraulic motor[17]

## 2. Establishment of geometric model of non-circular gear planetary gear train

### 2.1 Establishment of geometric model of higher-order ellipse planetary gear train

#### 2.1.1 Pitch Curve Design

The planetary gear train of the hydraulic motor with non-circular gears consists of a series of variable center distance NGW gear trains. These gear trains include sun gear, multiple planetary gears, and an inner ring gear. The sun gear and inner ring gear are non-circular, while the planetary gears are standard involuon cylindrical gears. Figure 2 illustrates their geometric motion relation. The polar equation  $R_1(\theta_1)$  of the solar gear node curve must satisfy the condition of uniform distribution of the gear teeth. According to the arc length formula, there are[9]:

$$\pi m z_1 = \int_0^{2\pi} \sqrt{R_1^2 + \left(\frac{dR_1}{d\theta_1}\right)^2} d\theta_1 \quad (1)$$

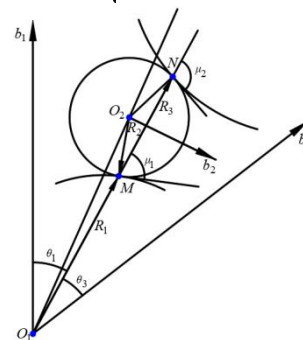


Figure 2. Geometric relationship of planetary gear train of non-circular gear hydraulic motor

To ensure continuous rotation of the non-circular gear hydraulic motor planetary gear system, the pitch curves of the sun gear and inner ring gear must be closed curves, satisfying the pitch curve closure condition [9]:

$$\frac{2\pi}{n_3} = \int_0^{2\pi} \frac{R_1 + 2R_2 \sin \mu_1}{R_1 + 2R_2 \sin \mu_1} \left(\frac{d\mu_1}{d\theta_1}\right) d\theta_1 \quad (2)$$

Where the expression for  $\mu_1$  is:

$$\tan \mu_1 = \frac{R_1}{\frac{dR_1}{d\theta_1}} \quad (3)$$

Based on the geometric relationship in Figure 2, the pitch curve of the non-circular planetary gear system is designed. There is the polar equation of the sun gear:

$$R_1 = \frac{A(1-k^2)}{1-k \cos(n_1\theta_1)} \quad (4)$$

The radius of the inner ring gear can be expressed as:

$$R_3 = R_1 + MN \tag{5}$$

$$MN = mR_2 \sin \mu_1 \tag{6}$$

Then the polar coordinate equation of the inner ring gear can be expressed as:

$$\begin{cases} R_3 = R_1 + mR_2 \sin \mu_1 \\ \theta_3 = \int_0^{\theta_1} \frac{R_1 + mR_2 \sin \mu_1 \left( \frac{d\mu_1}{d\theta_1} \right)}{R_1 + mR_2 \sin \mu_1} d\theta_1 \end{cases} \tag{7}$$

By solving equations (1) and (2), the values of  $A$  and  $k$  for the sun gear can be calculated. Then, by numerical analysis, equation (3) can be solved to obtain the polar coordinate numerical solution for the ring gear. When the parameters of the 6-8 type non-circular gear planetary gear train are set  $m=1.5$ ,  $z_1=66$  and  $z_2=10$ , pitch curve plotting is conducted using Matlab [18], as shown in **Figure 3**.

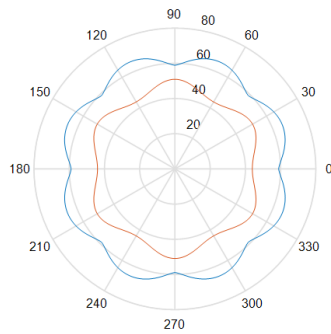


**Figure3.** High-order ellipse pitch curve of non-circular gear hydraulic motor

**2.1.2 Teeth profile design of high-order ellipse planetary gear train**

The teeth profile of the non-circular gear is generated using the gear tool's shape-generating motion. The teeth profile equation of the shape-generating gear is transformed to the gear coordinate system to obtain the envelope model of the teeth profile of the non-circular gear planetary gear train[19], as shown in **Figure 4**.

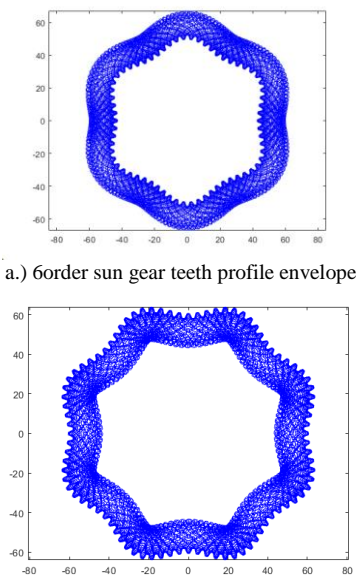


**Figure 4.** Higher-order ellipse envelope model of non-circular gear hydraulic motor

The teeth profile obtained is imported into the 3D modeling software for stretch modeling to obtain a higher-order ellipse 3D model of the planetary gear system of the non-circular gear hydraulic motor, as shown in **Figure 5**.



**Figure 5.** Non-circular gear hydraulic motor planetary geartrain high-order ellipse type 3D model

**2.2 Establishment of geometric model of double circular arc planetary gear train**

As an example, the planetary gear train of a non-circular gear hydraulic motor of type 6-8, in which the pitch curve in the form of a double circular arc of the inner ring gear of 8 order is shown in **Figure 6**. The whole pitch curve can be derived from the  $AB$  segment curve within  $0\sim 22.5^\circ$ , which is called the base curve. The base curve consists of two circular arc segments,  $AC$  and  $CB$ , with  $AC$  centered at  $O_1$  and  $CB$  centered at  $O_1'$ . Let the length of  $OO_1$  be  $x_1$ , the length of  $OO_1'$  be  $y_1$ , and the length of  $O_1C$  be  $r_1$ . Thus, for a fixed order of ellipse, the form of its pitch curve can be uniquely determined by three parameters:  $x_1$ ,  $y_1$ , and  $r_1$ .

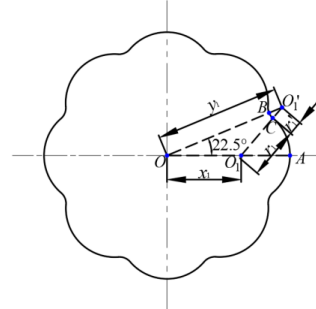


**Figure 6.** Double circular arc 8order inner ring gear pitch curve

The design must meet the following conditions:

**2.2.1 Arc length condition**

The sun gear and inner ring gear pitch curves of type 6-8 non-circular gear hydraulic motor are shown in **Figure 7**.

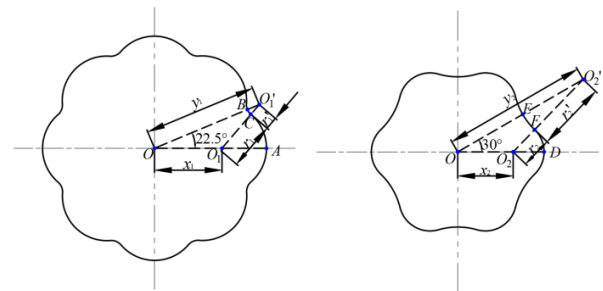


**Figure 7.** Double arc pitch curve of 6-8 type non-circular gear hydraulic motor

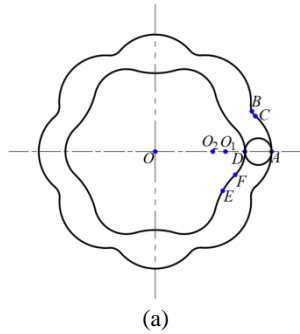
To ensure proper articulation of the gear teeth at points A, B, D, and E, the following arc lengths must be satisfied[14]:

$$L_{AC} + L_{CB} = \frac{K\pi m}{2} \tag{8}$$

$$L_{DF} + L_{FE} = \frac{K\pi m}{2} \tag{9}$$

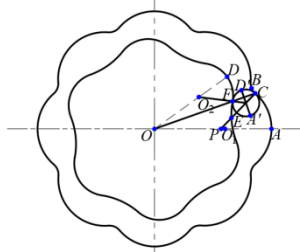
2.2.2 Transmission conditions

The non-circular gear hydraulic motor transmission of the planetary gear train has three special meshing positions, as shown in **Figure 8**. At special position 1, point A on the inner ring gear and point D on the sun gear align collinearly with the symmetry center O. At special position 2, point C on the inner ring gear and point F on the sun gear align collinearly with the symmetry center O. At special position 3, point B on the inner ring gear and point E on the sun gear align collinearly with the symmetry center O.

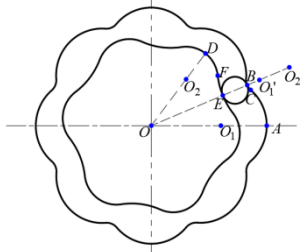


(a)

$$L_{AC} = L_{DF} + L_{FP} \tag{12}$$



(b)



(c)

a.) Special Position 1 b.) Special Position 2 c.) Special Position 3

**Figure 8.** Special meshing position of non-circular gear planetary gear train

Let  $r_3$  be the radius of the planetary gear, which can be obtained from the geometric relationship of special positions 1 and 3:

$$x_1 + r_1 = x_2 + r_2 + 2r_3 \tag{10}$$

$$y_1 + r_1' = y_2 - r_2' + 2r_3 \tag{11}$$

In Special Position 2, Point A' is the meshing point of Point A and Point D' is the meshing point of Point D. In this particular position, the three points A', D' and O<sub>3</sub> are collinear, because the meshing motion between the gears is purely rolling, so there are:

In addition, it can be seen from the collinearity of C, F and O:

$$\angle O_2FO = \angle FCO_3 \tag{13}$$

2.2.3 Constraint condition

In order to avoid teeth top interference in the running process of planetary gear train, it is necessary to meet the requirements[14]:

$$x_2 + r_2 < y_1 - r_1' \tag{14}$$

In order to avoid gear undercutting, meet the following requirements[14]:

$$\begin{cases} r_1 > 5m \\ r_1' > 5m \\ r_2 > 5m \\ r_2' > 5m \end{cases} \tag{15}$$

Therefore, the configuration of the pitch curve for the double circular arc type non-circular gear planetary gear train can be exclusively established by  $x_1, y_1, r_1, x_2, y_2$  and  $r_2$ . These six parameters must concurrently fulfill two arc length condition equations, four transmission condition equations, and five constraint conditions.

2.2.4 Pitch curve design method

The design of the pitch curve for a 6-8 non-circular gear planetary gear train can be transformed into a solution of a nonlinear programming model, according to the derivation [20] specific design method is as follows:

1.) Setting modulus  $m$  and  $K$  values. Given modulus  $m=1.5, K=11, z_3=10, r_3=7.5$ .

2.) Establishing nonlinear programming model. Assuming that the result of the calculation is  $[x_1, y_1, r_1, x_2, y_2, r_2]$ , the lower bound of the solution domain is  $[0, 0, 0, 0, 0, 0]$ , the upper bound of the solution domain is  $[10^4, 10^4, 10^4, 10^4, 10^4, 10^4]$ , and the initial value of the solution domain is  $[10, 10, 10, 10, 10, 10]$ . Equations (8) to (12) are used as equality constraints, equations (14) and (15) are used as inequality constraints, and equation (13) is used as objective function:  $f = |\angle FCO_3 - \angle O_2FO|$ .

3.) Solving the nonlinear programming model. The value of the objective function  $f$  at the minimum time  $[x_1, y_1, r_1, x_2, y_2, r_2]$  is solved using Matlab. The solution results are presented in **Table 1**.

**Table 1.** Result parameters

Parameters	Numerical value
$x_1$	39.5659
$y_1$	66.4284
$r_1$	25.9243
$x_2$	32.4735
$y_2$	84.8206
$r_2$	18.0844

4.) Drawing double arc pitch curve. Using AutoCAD to draw the pitch curve of planetary gear train of non-circular gear hydraulic motor, as shown in **Figure 9**.

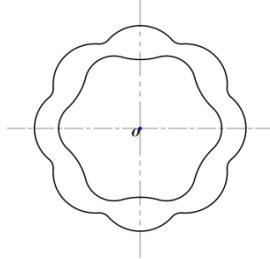


**Figure9.** Double circular arc pitch curve of planetary gear train of non-circular gear hydraulic motor

2.2.5 Double circular arc planetary gear train teeth profile design

**Figure 10** shows that the *AB* section of the inner ring gear serves as the base curve, from which corresponding involute teeth profiles are devised. Each teeth profile on the *AC* segment circular arc aligns with that of an internally meshing cylindrical gear with a radius of  $r_1$ , while each teeth profile on the *CB* segment circular arc corresponds to that of an externally meshing cylindrical gear with a radius of  $r_1'$ . Utilizing the teeth profile conversion technique, the actual gear teeth profile is converted into an equivalent standard gear shape. Subsequently, the teeth profile is graphed in CAXA, as depicted in **Figure 10**. The entire teeth profile is deduced from this segment, and the design methodology for the sun gear teeth profile follows a similar approach[21].

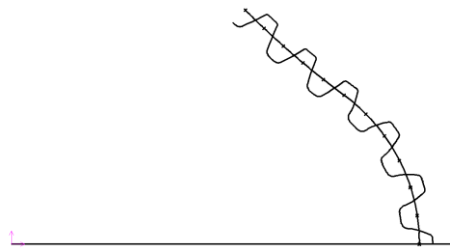


**Figure10.** Teeth profile design of inner ring gear

The teeth shape obtained is imported into the 3D modelling software for stretch modelling, resulting in a double circular arc type 3D model of the non-circular gear hydraulic motor planetary gear train, as shown in **Figure 11**.

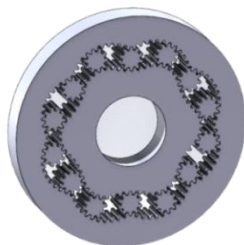


**Figure11.** Double circular arc 3D model of planetary gear train of non-circular gear hydraulic motor

3. Analysis of Transmission Performance of Non-circular Gear Hydraulic Motor

In the non-circular gear hydraulic motor planetary gear system, the transmission performance is mainly affected by the motion characteristics, flow distribution characteristics pulsation coefficient and other factors. These factors together determine the transmission efficiency, stability, noise and service life of the motor[22].The paper has analyzed the transmission performance aspects of a non-circular gear hydraulic motor model obtained from two different modeling methods.

3.1 Motion characteristic analysis

The motion of the planetary gear train during transmission in the non-circular gear planetary gear system can be considered as planar motion. This motion is composed of two parts: rotation around the centre of the sun gear and rotation around its own axis.

Various modelling approaches lead to variations in the kinematic features of non-circular gear planetary gear trains. The rotational speed of the planetary gear and the magnitude of the rotational angle determine the impact force during the rotation process. The centrifugal force produced in the planetary gear rises with the rotational angle speed, leading to increased wear and tear between the planet gear, the inner ring gear, and the sun gear. This reduces the transmission performance and stability of the entire mechanism, and also increases the noise[23]. The use of the higher-order ellipse non-circular gear hydraulic motor's planetary gear train, as an example, shows that the velocity of the planetary gear's centroid can be deduced from the geometric motion relationship in **Figure 2**.

$$v_{o_2} = \frac{dr_{o_2}}{dt} \tag{16}$$

$$v_{o_2} = r_{o_2} \frac{d\phi_{o_2}}{dt} \tag{17}$$

The angular velocity of planetary gear  $\omega_2$  is:

$$\omega_2 = \omega_1 \frac{\phi'_2}{\phi'_1} \tag{18}$$

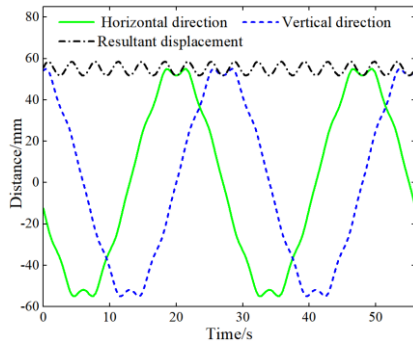
Equations (16) to (18) contain the following parameters:

$$r_{o_2} = \sqrt{R_1^2 + R_2^2 + 2R_1R_2 \sin \mu_1} \tag{19}$$

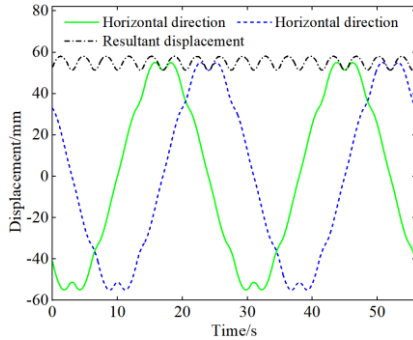
$$\phi_{o_2} = \theta_3 + \arctan \left( \frac{R_2 \cos \mu_1}{R_1 + R_2 \sin \mu_1} \right) \tag{20}$$

With carbon steel as the material of the motor planetary gear train, the angular velocity of the sun gear  $\omega_1$  is 30 rad/s, the direction is counterclockwise, and the load is applied to the center of the sun gear. According to the dynamic relationship, the contact between the sun gear and the planetary gear is used to drive the planetary gear. The displacement, speed and rotation velocity of the planetary gear can be derived from the rotation velocity of the sun gear. The double circulararc model can also be analyzed using the same method to compare the rotational displacement, rotational velocity, and rotational angular velocity of the planetary gear as shown in **Figure 12 to 14**.



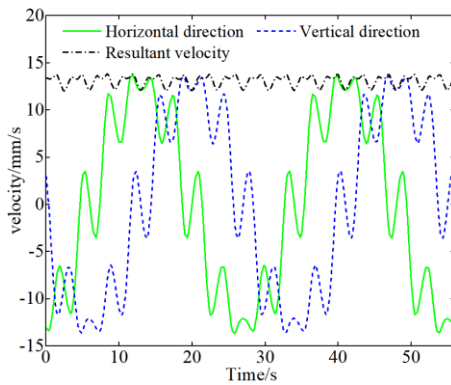


a.) Displacement of centroid of planetary gears of higher-order ellipse motors

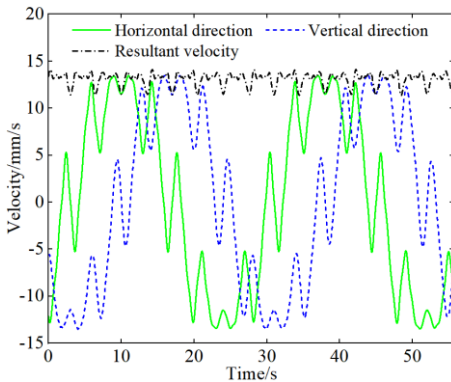


b.) Displacement of the centroid of the planetary gear of a double circular arc motor

**Figure 12.** Centroid displacement of planetary gears of two motors



a.) Centroid velocity of planetary gear of higher-order ellipse motor



b.) Centroid velocity of planetary gear of double circular arc motor

**Figure 13.** Centroid velocities of planetary gears of two motors

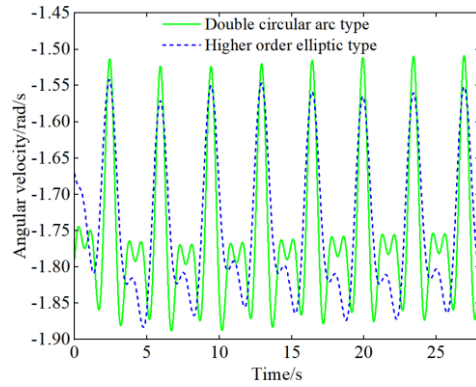


**Figure 14.** Rotation angular velocity of planetary gears of two motors

As shown in **figures 12 to 14**, the trajectory of the center of the planetary gear in a non-circular gear planetary gear train is periodic. The speed and rotational angular speed also exhibit periodicity and remain continuous within each cycle. The velocity and rotational angular velocity of the planetary gear change at the maximum and minimum diameters of the inner ring gear. The timing and period of the speed change of the planetary gear coincide with those of the change in rotational angular velocity. This condition is due to the unique geometry of the non-circular gear and the relative motion of the planetary gear at different positions. When the planetary gear moves to the arc with a larger radius of the inner ring gear, the rotational angular velocity of the planetary gear changes little but the average speed changes more. As the planetary gear moves to the arc with a small radius of the inner ring gear, the rotational angular velocity of the planetary gear changes greatly but the average speed changes little.

### 3.2 Analysis of flow distribution characteristics

As illustrated in **Figure 15**, the volume of the confined chamber, which is surrounded by the sun gear, the inner ring gear, and the planetary gears 1 and 2, reaches its maximum when the sun gear is in the position indicated by the black line. Conversely, when the sun gear is turned clockwise to the position indicated by the blue line, the volume of the confined chamber reaches its minimum. At maximum volume, the root circle of planetary gear 2 tooth should be positioned to just open the outlet port. Therefore, the circular position where the planetary gear 2 intersects with the planetary gear 1' is the oil outlet hole, indicated by the red line. The oil holes and outlet holes are collectively referred as the distribution holes, and the circular area shown by the red line is the area of the distribution holes.

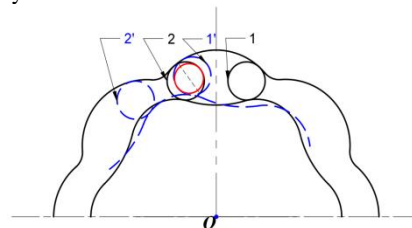


**Figure 15.** Schematic diagram of flow distribution hole positioning

The locations of the other in and outflow distribution holes can also be determined using the same method. In the case of a shaft type motor where the sun gear rotates but the housing does not, there are a total of  $n_3$  inlet holes and  $n_3$

outlet holes, as total  $2n_3$  flow distribution holes [24]. The 6-8 type non-circular gear hydraulic motor has 16 flow distribution holes, with 8 inlet and 8 outlet holes. The radius of the distribution hole and the position of the center of the distribution hole can be calculated according to the geometric relationship of the tangent circle, and the specific data are shown in **Table 2**.

**Table 2.** Parameters of distribution hole

[1] Model	[2] Radius of flow distribution hole	[3] Distance between the center of flow distribution hole and the center of motor
[4] High order ellipse type	[5] 5.837mm	[6] 55.496mm
[7] Double circular arc type	[8] 5.784mm	[9] 54.979mm

As shown in **Figure 16**, not all chambers are working chambers during the operation of a non-circular gear hydraulic motor. The 14 confined cavities are numbered sequentially, and from the average transmission ratio, the critical position of oil inlet and discharge occurs at the least common multiple of the sun gear rotation angles of  $2\pi/n_1$  and  $2\pi/n_3$ . In the motor working process, the motor each oil chamber working state exists symmetrical relationship, in and out of the oil rule as shown in **Table 3**.

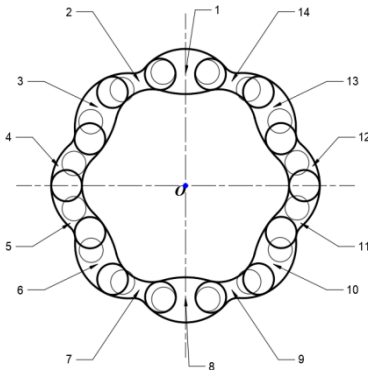


**Figure 16.** Distribution map of port hole

**Table 3** shows the different states of the chamber: oil in (+), oil out (-), maximum area and preparation for oil discharging 'Critical -', and minimum area and preparation for oil feeding 'Critical +'. When the cavity is at its maximum area and ready to discharge oil, it is

referred to as 'Critical -'. Conversely, when the cavity is at its minimum area and ready to feed oil, it is referred to as 'Critical +'. It can be seen that when the sun gear rotates  $105^\circ$  each cavity to complete a complete cycle of oil in and out of a cycle. In a cycle, the cavity follows the six rows of two critical or eight into the six rows of six, six into the eight rows of the rule.

**3.3 Displacement and stability analysis**

Displacement refers to the volume of fluid passing through the motor during one revolution of the output shaft[25]. Following the aforementioned distribution pattern, the volume variation of each enclosed chamber adheres to the same pattern. Therefore, analyzing just one of them is sufficient.

When the planetary gear meshes with the inner ring gear and the sun gear, the cavity area can be fitted by the pitch curve. As shown in **Figure 17**, the green line represents the pitch circle of the planetary gear, and the areas of the two parts marked "1" and "2" are considered to be approximately equal, which is the area of the gear outside the pitch circle that can supplement the area fitted inside the pitch circle. Therefore, the area of the cavity is only related to the pitch circle of the planetary gear, the pitch curve of the inner ring gear and the sun gear, and the equivalent area can be calculated by the pitch curve fitting method.

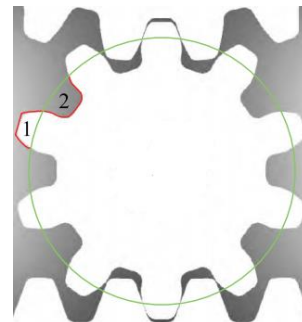


**Figure 17.** Diagram of equivalent area of gear meshing

As depicted in **Figure 18**, when the smallest diameter of the sun gear coincides with the largest diameter of the inner ring gear, the chamber volume is maximized, conversely, when the largest diameter of the sun gear aligns with the smallest diameter of the inner ring gear, the chamber volume is minimized. During the operation of the non-circular gear hydraulic motor, the volume of each closed chamber changes constantly with the rotation angle of the sun gear. This causes a corresponding change in the inhaled and discharged oil.

**Table 3.** Oil inlet and outlet rule of closed cavity

Rotation angle of sun gear/ $^\circ$	Closed chambers 1 and 8	Closed chambers 2 and 9	Closed chambers 3 and 10	Closed chambers 4 and 11	Closed chambers 5 and 12	Closed chambers 6 and 13	Closed chambers 7 and 14
0	Critical-	+	-	+	-	+	-
17.5	-	+	-	+	-	+	-
35	-	+	-	-	+	+	-
52.5	Critical+	-	+	-	+	-	+
70	+	-	+	-	+	-	+
87.5	+	-	+	+	-	-	+
105	Critical-	+	-	+	-	+	-

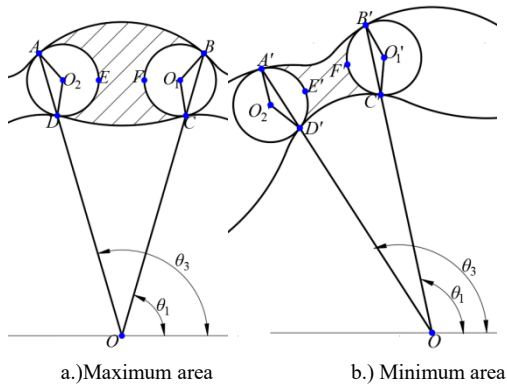


Figure 18. Schematic diagram of motor displacement

By calculating the minimum and maximum area of the sealed cavity in the drafting software and simultaneously changing the sun gear rotational angle, the relationship between the sun gear angle and the change in cavity area is obtained, as shown in Figure 19.

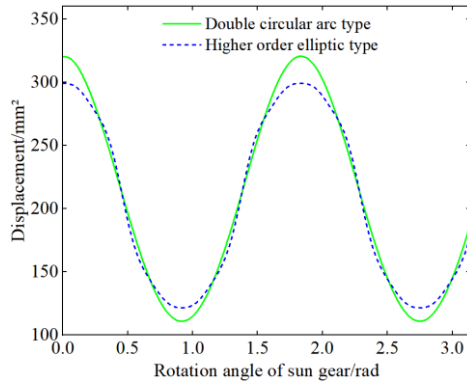


Figure 19. Comparison of displacement in the same cavity between two motor models

Figure 19 shows that under the same parameters, the double circular arc non-circular gear hydraulic motor can intake and discharge more oil during the same chamber working cycle compared to the higher-order ellipse hydraulic motor. Consequently, the double circular arc non-circular gear hydraulic motor achieves a higher displacement per unit time than the higher-order ellipse hydraulic motor. This phenomenon arises due to differences in design and working principles between the double circular arc motor and higher-order ellipse motor. The double circular arc motor, through its specialized pitch curve design, can more effectively propel oil flow, resulting in a larger displacement during a chamber's working cycle. Conversely, the higher-order ellipse hydraulic motor exhibits relatively weaker performance under the same design parameters.

The stability of a non-circular gear hydraulic motor is determined by the pulsation coefficient of displacement [26], which refers to the rate of change of the volume of oil input into the motor at any given moment. A lower pulsation coefficient corresponds to higher stability of the motor at that instant. The pulsation rate of displacement is defined by the following equation:

$$\delta_q = \frac{q_{max} - q_{min}}{q_{av}} \quad (21)$$

Equation (21) shows that the instantaneous chamber is in the oil intake state when  $\delta_q > 0$  and in the oil discharge

state when  $\delta_q < 0$ . As indicated by the results in Figure 20. At the same level, the non-circular gear hydraulic motor with a double arc type has a smaller displacement pulsation rate. This type of motor is more stable during the oil inlet and discharge process, resulting in reduced vibration and noise. Therefore, the double circular arc type non-circular gear hydraulic motor is superior in terms of average displacement and running smoothness.

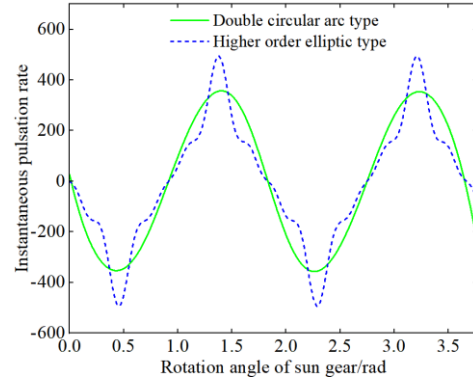


Figure 20. Comparison of displacement pulsation rate of two motor models in the same cavity

#### 4. Conclusion

For the planetary gear system of 6-8 type non-circular gear hydraulic motors using different modeling methods, the transmission performance was analyzed, and the conclusions are as follows:

1. The results show that the centroid speed and self-rotation angular speed of the planetary gears fluctuate periodically, and both have coinciding fluctuation periods. These fluctuations occur at the positions where the radial diameter of the internal gear ring is maximum. The occurrence of these fluctuations is related to the unique geometric shapes of the non-circular gears and the relative motion of the planetary gears at different positions. When the planetary gear moves to the arc with a larger radius of the inner ring gear, the rotational angular velocity of the planetary gear changes little but the average speed changes more. As the planetary gear moves to the arc with a small radius of the inner ring gear, the rotational angular velocity of the planetary gear changes greatly but the average speed changes little.
2. During the operation of a hydraulic motor, not all of its chambers are operational. Both modeling methods of the 6-8 type non-circular gear hydraulic motor follows the six into the six rows of two critical or eight into the six rows of six, six into the eight rows of the rule. These changes are caused by the rotation angle of the sun gear, which affects the volumes of the chambers and manifests in the pulsation rate of displacement. During the operation of the hydraulic motor, the volumes of the enclosed chambers change at different intervals, resulting in fluctuations in the overall displacement.
3. The analysis shows that under identical conditions, the double circular arc non-circular gear hydraulic motor demonstrates a higher capacity to intake and discharge oil volume during the same chamber working cycle in comparison to the high-order ellipse non-circular gear hydraulic motor. Consequently, in displacement terms, the double circular arc non-circular gear hydraulic motor



outperforms the higher-order ellipse non-circular gear hydraulic motor. Furthermore, when contrasted with the higher-order ellipse non-circular gear hydraulic motor, the double circular arc non-circular gear hydraulic motor exhibits superior performance in both displacement and operational stability.

### Acknowledgement

This research gained sponsorship from The National Natural Science Foundation of China (No.52265008), the Gansu Province Youth Science Foundation Project of China (Grant No. 23JRR751), the Gansu Provincial Department of Education of China: Innovation Fund Project for University Teachers (Grant No. 2023A-021).

### Reference

- [1] D. Nie, C. Fu. "The Application of Closed Hydraulic System of Hoisting Mechanism in Auto Crane". *Jordan Journal of Mechanical and Industrial Engineering (JJMIE)*, vol. 14, no. 1, 2020, pp. 37-41.  
<https://jjmie.hu.edu.jo/VOL-14-1/05-jjmie-437-01.pdf>.
- [2] G. Yu, D. Fadyushin. "Improvement of the method of geometric design of gear segments of a planetary rotary hydraulic machine". *Journal of Physics: Conference Series*, Vol. 1889, No. 4, 2021, pp. 042-052.  
<https://doi.org/10.1088/1742-6596/1889/4/042052>.
- [3] B. Li, D. Chen. "Design, Manufacture, Inspection and Application of Non-circular Gears". *Journal of Mechanical Engineering*, Vol. 56, No. 09, 2020, pp. 55-72.  
<https://doi.org/10.3901/JME.2020.09.055>.
- [4] A. Al-Shyyab, A. Kahraman, A. Jawarneh, H. Thilan. "Non-linear Dynamic Behaviour of Compound Planetary Gear Trains: Model Formulation and Semi-Analytical Solution". *Proc. IMechE, Part K: Journal of Multi-body Dynamics*, Vol. 223, No.3, 2009, pp. 199-210.  
<https://doi.org/10.1243/14644193JMBD197>.
- [5] A. Al-Shyyab, A. Kahraman, A. Kahraman. "Nonlinear Torsional Dynamic Model of Multi-Mesh Gear Trains Having Flexible Shafts". *Jordan Journal of Mechanical and Industrial Engineering (JJMIE)*, Vol. 1, No. 1, 2007, pp. 31-41.  
<https://jjmie.hu.edu.jo/files/005.pdf>.
- [6] C. Dong, Y. Liu, X. Fu, C. Dou, Y. Yin. "Research on the Effect of Rotation Speed on the Meshing Characteristics of Elliptical Cylindrical Gears". *Jordan Journal of Mechanical and Industrial Engineering (JJMIE)*, Vol. 14, No. 3, 2020, pp. 221-227.  
<https://jjmie.hu.edu.jo/vol14-3/01-09.pdf>.
- [7] A. Hammood. "Towards Condition Monitoring: Fabrication and Finite Element Analysis of a Helical Gear Transmission Rig for Fault Simulation". *Jordan Journal of Mechanical and Industrial Engineering (JJMIE)*, Vol. 18, No. 1, 2024, pp. 219-226.  
<https://doi.org/10.59038/jjmie/180117>.
- [8] R. Jasiński. "Analysis of the Heating Process of hydraulic motors during start-up in thermal shock conditions". *Energies*, Vol. 15, No. 1, 2021, pp. 55-55.  
<https://doi.org/10.3390/en15010055>.
- [9] B. Zhang, S. Song, C. Jing, et al. "Displacement prediction and optimization of a non-circular planetary gear hydraulic motor". *Advances in Mechanical Engineering*, Vol. 13, No. 11, 2021, pp. 1-13.  
<https://doi.org/10.1177/16878140211062690>.
- [10] P. Sliwinski. "The methodology of design of satellite working mechanism of positive displacement machine". *Scientific reports*, Vol. 12, No. 1, 2022, pp. 13685-13685.  
<https://doi.org/10.1038/s41598-022-18093-z>.
- [11] P. Sliwinski. "Influence of geometrical and operational parameters on tooth wear in the working mechanism of a satellite motor". *Scientific Reports*, Vol. 13, No. 1, 2023, pp. 17028-17028.  
<https://doi.org/10.1038/s41598-023-44319-9>.
- [12] P. Sliwinski. "Geometric working volume of a satellite positive displacement machine". *Scientific Reports*, Vol. 14, No. 1, 2024, pp. 11195-11195.  
<https://doi.org/10.1038/s41598-024-61773-1>.
- [13] N. Shi, Q. Liu, Q. Li, et al. "Three-dimensional parametric modeling method of non-circular planetary gear hydraulic motor". *Journal of Ordnance Equipment Engineering*, Vol. 44, No. 02, 2023, pp. 234-240.  
<https://doi.org/10.11809/bqzbgcxb2023.02.0350>.
- [14] D. Li, Y. Liu, J. Gong, et al. "Design of a non-circular planetary gear mechanism for hydraulic motor". *Mathematical Problems in Engineering*, Vol. 2021, 2021.  
<https://doi.org/10.1155/2021/5510521>.
- [15] C. Song, X. Li, Y. Yang, J. Sun, et al. "Parameter design of double circular arc teeth profile and its influence on meshing characteristics of harmonic drive". *Mechanism and Machine Theory*, Vol. 167, 2022.  
<https://doi.org/10.1016/j.mechmachtheory.2021.104567>.
- [16] W. Zhang, Y. Wang, K. Zhang, et al. "Design and feasibility study of Downhole all-metal non-circular gear power drilling tools". *Geology and Exploration*, Vol. 59, No. 01, 2023, pp. 154-161.  
<https://doi.org/10.12134/j.dzykt.2023.01.013>.
- [17] P. Sliwinski. "SATELLITE PUMP AND MOTOR". *International Scientific Journals*, Vol. 8, No. 9, 2014, pp. 8-11.  
<https://stumejournals.com/journals/mtm/2014/9/8>.
- [18] Q. Xu, C. Yang, J. Zhao, et al. "Modeling of Non-circular Gear Mechanism Based on Reverse Engineering Technology". *Machine Tool & Hydraulics*, Vol. 47, No. 05, 2019, pp. 136-139.  
<https://doi.org/10.3969/j.issn.1001-3881.2019.05.031>.
- [19] Y. Liu, B. Yuan, Y. Wei, et al. "Research on digital design and teeth profile optimization of non-circular gear based on envelope feature". *Journal of Mechanical Transmission*, Vol. 46, No. 08, 2022, pp. 55-60.  
<https://doi.org/10.16578/j.issn.1004.2539.2022.08.009>.
- [20] N. Ebenezer, S. Ramabalan, S. Navaneethasanthakumar. "Advanced Multi Criteria Optimal Design of Spiral Bevel Gear Pair using NSGA - II". *Jordan Journal of Mechanical and Industrial Engineering (JJMIE)*, Vol. 16, No. 2, 2022, pp. 185-193.  
<https://jjmie.hu.edu.jo/vol16-2/03-55-21.pdf>.
- [21] M. Tomova, B. Prangoskia, P. Karolczak. "Mathematical Modelling and Correlation Between the Primary Waviness and Roughness Profiles During Hard Turning". *Jordan Journal of Mechanical and Industrial Engineering (JJMIE)*, Vol. 15, No. 3, 2021, pp. 243-249.  
[https://jjmie.hu.edu.jo/V15-3/01-jjmie\\_23\\_21.pdf](https://jjmie.hu.edu.jo/V15-3/01-jjmie_23_21.pdf).
- [22] E. Rezaei, M. Poursina, M. Rezaei, A. Ariaei. "A New Analytical Approach for Crack Modeling in Spur Gears". *Jordan Journal of Mechanical and Industrial Engineering (JJMIE)*, Vol. 13, No. 2, 2019, pp. 69-74.  
[https://jjmie.hu.edu.jo/vol-13-2/jjmie\\_36\\_19-01.pdf](https://jjmie.hu.edu.jo/vol-13-2/jjmie_36_19-01.pdf).
- [23] Y. Liu, X. Fu, Y. Wei, et al. "Parametric design and motion simulation analysis of non-circular gear planetary gear train". *Journal of Mechanical Transmission*, Vol. 45, No. 08, 2021, pp. 70-75.  
<https://doi.org/10.16578/j.issn.1004.2539.2021.08.010>.
- [24] P. Sliwinski. "The methodology of design of axial clearances compensation unit in hydraulic satellite displacement

machine and their experimental verification".Archives of Civil and Mechanical Engineering,Vol. 19, No. 4, 2019, pp. 1163-1182.

<https://doi.org/10.1016/j.acme.2019.04.003>.

- [25] P. Sliwinski."Influence of operating pressure on the durability of a satellite hydraulic motor supplied by rapeseed oil".Scientific reports,Vol. 14, No. 1, 2024, pp. 10441-10441.

<https://doi.org/10.1038/s41598-024-61072-9>.

- [26] Y. Liu, X. Li. "Analysis of speed and stability of non-circular gear hydraulic motor".Heavy Machinery, No. 1, 2023, pp. 27-33.

<https://doi.org/10.13551/j.cnki.zxjqk.2023.01.005>.